

Observation of Nonlinear Response and Onsager Regression in a Photon Bose-Einstein Condensate

Alexander Sazhin ¹, Vladimir N. Gladilin ², Andris Erglis ³, Göran Hellmann ^{1,*}

Frank Vewinger ¹, Martin Weitz ¹, Michiel Wouters ² and Julian Schmitt ^{1,†}

¹*Institut für Angewandte Physik, Universität Bonn, Wegelerstr. 8, 53115 Bonn, Germany*

²*TQC, Universiteit Antwerpen, Universiteitsplein 1, B-2610 Antwerpen, Belgium*

³*Physikalisches Institut, Albert-Ludwigs-Universität Freiburg, Hermann-Herder-Straße 3, 79104, Freiburg, Germany*

(Dated: March 18, 2024)

The quantum regression theorem states that the correlations of a system at two different times are governed by the same equations of motion as the temporal response of the average values. Such a relation provides a powerful framework for the investigation of physical systems by establishing a formal connection between intrinsic microscopic behaviour and a macroscopic "effect" due to an external "cause". Measuring the response to a controlled perturbation in this way allows to determine, for example, structure factors in condensed matter systems as well as other correlation functions of material systems. Here we experimentally demonstrate that the two-time particle number correlations in a photon Bose-Einstein condensate inside a dye-filled microcavity exhibit the same dynamics as the response of the condensate to a sudden perturbation of the dye molecule bath. This confirms the regression theorem for a quantum gas and, moreover, establishes a test of this relation in an unconventional form where the perturbation acts on the bath and only the condensate response is monitored. For strong perturbations, we observe nonlinear relaxation dynamics which our microscopic theory relates to the equilibrium fluctuations, thereby extending the regression theorem beyond the regime of linear response. The demonstrated nonlinearity of the condensate-bath system paves the way for studies of novel elementary excitations in lattices of driven-dissipative photon condensates.

The application of linear response theory to systems that are subject to perturbations lies at the heart of many fundamental phenomena in physics [1], including electromagnetic wave propagation in optical media, structure factors in condensed matter systems, or superfluid phases in quantum gases [2–4]. For strong perturbations, the extension of this concept to nonlinear response has facilitated our understanding of ubiquitous effects such as higher-harmonic generation in optics [5] or the emergence of turbulent flow in cold-atom and exciton-polariton systems driven far from equilibrium [6, 7]. When considering equilibrium systems, the linear response behaviour is commonly governed by the fluctuation-dissipation theorem [8], which states that the intrinsic fluctuations of a system are connected to the absorptive part of a response function by thermal energy. The Onsager-Lax theorem, covering situations where the magnitude of the fluctuations is small, remains valid also for systems out of equilibrium and describes a universal relationship between the correlations and the response dynamics, as has been theoretically shown for irreversible processes in classical and quantum systems [9–17]. The usual regression theorem, which states that the two-time averages $\langle A(t)B(0) \rangle$ of two observables A and B obey the same equations as the one-time averages $\langle A(t) \rangle$ for Markovian systems [12], links the system's fluctuations to the linear response, but more recent works have theoretically addressed nonlinear response as well [18]. Experimentally, it has been indirectly verified by measurements of Onsager's reciprocity relations in the classical domain, *e.g.*, in thermoelectric systems or thin films [19, 20]. A direct experimental test of this central theorem of statistical physics, however, by independent measurements of the temporal response to a perturbation and of the system's fluctuation dynamics has so far not been carried out for quantum gas systems [21–23].

To examine the regression theorem for a quantum gas, we investigate the reservoir-induced dynamics of a Bose-Einstein condensate (BEC) of photons in a dye-filled optical microcavity. In the used experimental platform, a two-dimensional photon gas is coupled radiatively to a reservoir of dye molecules [24–26]. Previous work has, by observing the statistical number fluctuations that result from an effective particle exchange with the molecular reservoir, reported a non-Hermitian phase transition [27, 28], verified a fluctuation-dissipation relation connected to a reactive response function [29], and realised protocols to temporally perturb the reservoir [30, 31]. Moreover, theory work on this system has employed the regression theorem to calculate two-point correlations from the relaxation dynamics [32, 33].

Figure 1a illustrates how a photon BEC couples to a reservoir of dye molecules, providing a benchmarking platform for the regression theorem in complex many-body quantum systems of both matter and light. In a unique fashion, the system allows one to connect the linear response dynamics after a weak perturbation (Fig. 1a, left panel) with the intrinsic fluctuations driven by coloured noise (Fig. 1a, middle) and with the nonlinear response after a strong perturbation (Fig. 1a, right). Unlike the more usually encountered situation for the quantum regression theorem where a system (here the BEC) itself is perturbed, the perturbation here acts on the reservoir part (molecules), the excitation is transferred to the system by light-matter interactions (illustrated by a spring), and only then the photon number dynamics is witnessed by an observer before it is damped out by dissipation of photons to the environment. Despite its microscopic complexity, at the mean-field level the photon-molecule system can effectively be described as a damped harmonic oscillator, which exhibits a pronounced nonlinearity for large perturbations.

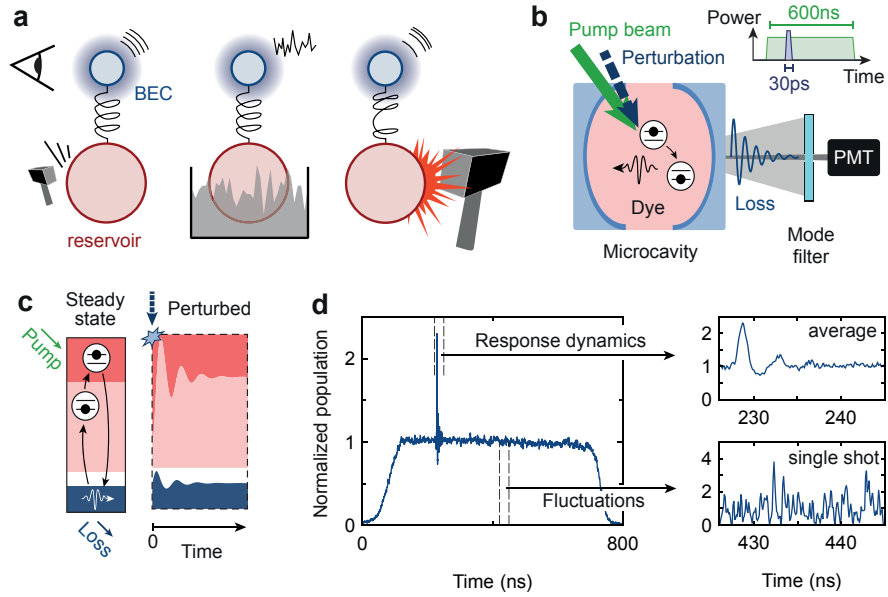


Fig. 1. Experimental scheme to probe the regression theorem. **a**, Mechanical analogue of a photon Bose-Einstein condensate (top, blue) coupled to a molecule reservoir (bottom, red), forming a quantum dissipative oscillator. A weak sudden perturbation of the reservoir (left) leads to a linear response of the average single-time photon number $\langle n(t) \rangle$. Immersion into a “coloured-noise” bath (middle) leads to number fluctuations δn , or alternatively, two-time correlations $\langle \delta n(t) \delta n(0) \rangle$, for which the regression theorem predicts the same dynamics. For a strong perturbation (right), the response becomes nonlinear. **b**, Dye-filled optical microcavity with photon Bose-Einstein condensate, which is perturbed by a laser pulse irradiated on the dye reservoir (inset). The fluctuation and response dynamics are recorded on a photomultiplier (PMT). **c**, In a steady state, when cavity losses are compensated by pumping the dye, photons (blue) and molecules in the ground and excited state (red) are in equilibrium due to absorption and emission events. After a sudden perturbation of the excited molecules, also the condensate population is perturbed and both systems relax back to their stationary values. **d**, *Left*: Temporal evolution of the condensate averaged over several time traces. *Right*: Zoom-in on photon number response dynamics (top), exemplary single-shot time trace with fluctuations (bottom).

In this study, we measure the nonequilibrium response dynamics of a photon Bose-Einstein condensate after a sudden perturbation of its equilibrium dye reservoir. By comparing the response to the independently measured number fluctuations of the condensate, we first experimentally confirm the validity of the regression theorem for the optical quantum gas in the limit of weak perturbations. Further, for stronger perturbations we observe the emergence of nonlinear dynamics that is attributed to the saturation of the particle reservoir. Notably, the seemingly violated regression theorem is fully restored by a theoretical model that captures the nonlinear response dynamics, whose relevant parameters are the same as in the linear response. Such a nonlinearity in the condensate-bath system, which has been theoretically predicted also for exciton-polariton systems [34], forms the basis for future studies into the properties of elementary and topological excitations within lattices of photon condensates [35–37].

Our photon Bose-Einstein condensates are prepared inside an optical microcavity filled with a dye solution of refractive index $\tilde{n} \approx 1.44$ and concentration 1 mmol L^{-1} , see Fig. 1b; for details see Ref. [32] and Methods. The microcavity is formed by two spherical mirrors with a reflectivity $> 99.998\%$ and 1 m radius of curvature. At the used microcavity length $D_0 \approx 1.5 \mu\text{m}$, the free spectral range of the cavity becomes as large as the emission and absorption spectral profiles of the dye medium, which restricts the photon dy-

namics to the two transverse degrees of freedom at a fixed longitudinal mode number $q = 7$. Inside the microcavity, the photons behave as a two-dimensional gas of bosons with effective mass $m_{\text{ph}} = \pi \hbar q \tilde{n} / (D_0 c) \approx 10^{-35} \text{ kg}$ and quadratic dispersion; the minimum photon energy $m_{\text{ph}}(c/\tilde{n})^2 = \hbar \omega_c \approx 2.1 \text{ eV}$ is given by the energy of the transverse ground mode. In addition, the mirror curvature induces a harmonic trapping potential of frequency $\Omega/(2\pi) \approx 40 \text{ GHz}$ for the photons. The emission and absorption rates $B_{\text{em}}(\omega)$ and $B_{\text{abs}}(\omega)$ of the dye medium at $T = 300 \text{ K}$ fulfil the Kennard-Stepanov relation $B_{\text{em}}/B_{\text{abs}} \propto \exp(-\hbar\Delta/k_B T)$, which depends on the detuning $\Delta = \omega - \omega_{\text{zpl}}$ of the photon frequency from the zero-phonon line ω_{zpl} [27]. By absorption-emission cycles with dye molecules (10^{-12} s timescale), the photons thermalise to the rovibronic temperature of the dye before leaving the cavity (10^{-9} s). Above the critical photon number $N_c = \pi^2/3(k_B T/\hbar\Omega)^2 \approx 80000$, the photon gas exhibits Bose-Einstein condensation [24–26]. Despite the thermalisation mechanism, the photon Bose-Einstein condensate realises a weakly-dissipative macroscopic quantum system due to losses, *e.g.*, from photons leaking through the cavity mirrors. To establish a steady state of photons and molecules, the dye medium is externally pumped.

Under steady-state conditions, the weakly-dissipative character of the open condensate system is evident from an exceptional point in the second-order temporal correlations [28].

The underlying stochastic number fluctuations are caused by an effective particle exchange between the condensate and a large reservoir of excited molecules [27]. In the present work, we access the open-system dynamics of the condensate by investigating the photon number response after a controlled sudden perturbation of this reservoir. This allows us to test the validity of the regression theorem for the optical quantum gas, as well as to explore the regime of beyond-linear response. To begin with, we derive an analytical expression for the response dynamics [38] from two coupled rate equations for the number of photons n and excitations $X = n + M_{\uparrow}$, respectively, given by $dn/dt = B_{\text{em}}M_{\uparrow}(1+n) - B_{\text{abs}}M_{\downarrow}n - \kappa n$ and $dX/dt = PM_{\downarrow} - \kappa n - \Gamma_{\text{sp}}M_{\uparrow}$ (Methods). Here $M_{\downarrow,\uparrow}$ denotes the number of molecules in their ground (\downarrow) and electronically excited (\uparrow) states, P the pump rate, κ the cavity loss rate, and Γ_{sp} the spontaneous decay rate to unconfined modes. A steady state is established if the losses are compensated for by a constant pumping of rate $P = \kappa\langle n \rangle + \Gamma_{\text{sp}}\langle M_{\uparrow} \rangle / \langle M_{\downarrow} \rangle$, where $\langle \dots \rangle$ denotes temporal averaging, see Fig. 1c.

A time-dependent perturbation $P(t)$ of the molecule reservoir, however, drives the photon condensate away from the steady state. The resulting photon number evolution $n(t) = \langle n \rangle \exp\{B_{\text{em}}[1 + \exp(\hbar\Delta/k_{\text{B}}T)] \int_0^t m(t')dt'\}$ depends on the strength of the perturbation and therefore on the deviation $m(t)$ of the excited molecule number from the steady state number that would correspond to the instantaneous photon number $n(t)$. As detailed in the Methods, approximating the time integral over the perturbed molecules yields a nonlinear expression for the photon number response $R(t) = n(t) - \langle n \rangle$:

$$R(t) = \langle n \rangle \exp \left[B_{\text{em}}(1 + e^{\frac{\hbar\Delta}{k_{\text{B}}T}}) m_0 \frac{e^{s_+t} - e^{s_-t}}{s_+ - s_-} \right] - \langle n \rangle \quad (1)$$

Here $m_0 = m(0)$ gives the number of molecules excited by the initial pulse perturbation at $t = 0$. The eigenvalues $s_{\pm} = -\delta \pm \sqrt{\delta^2 - \omega_0^2}$ depend on the system parameters $\Delta, B_{\text{em}}, T, \Gamma_{\text{sp}}, \kappa$, molecule number M , and the steady-state photon number $\langle n \rangle$, where the damping rate δ and the oscillation frequency ω_0 determine whether a biexponentially damped ($\delta > \omega_0$) or an oscillatory ($\delta < \omega_0$) response is expected. Expanding eq. (1) yields a linear expression for the response $R(t) \simeq \langle n \rangle B_{\text{em}}[1 + \exp(\hbar\Delta/k_{\text{B}}T)] m_0 (e^{s_+t} - e^{s_-t}) / (s_+ - s_-)$. Both expressions are used to analyse the response dynamics, but eq. (1) describes the measured response more accurately in the regime of strong perturbations. The expected second-order coherence at time delay τ on the other hand can, by utilizing the regression theorem, be written as $g^{(2)}(\tau) \propto (s_+e^{s_+\tau} - s_-e^{s_-\tau}) / (s_+ - s_-) \propto dR(\tau)/d\tau$ (see Methods). Physically, the derivative follows from the fact that it takes some time for the molecules excited by the laser pulse to be converted into photons. This gives a delay for the response function with respect to the correlation function, in contrast to a direct perturbation of the photon number. Unlike the response, the fluctuation dynamics $g^{(2)}(\tau)$ is intrinsically linear due to the grand canonical condition for large fluctuations being realised only for large reservoirs which basically cannot be saturated.

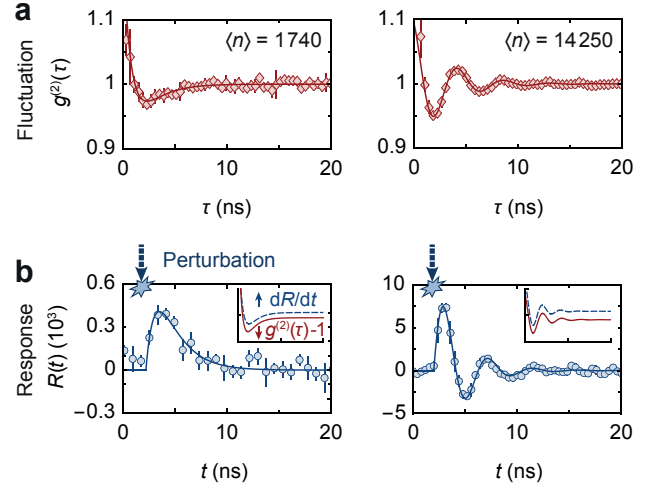


Fig. 2. Fluctuation and response dynamics. **a**, Second-order correlation functions $g^{(2)}(\tau)$ for steady-state photon numbers $\langle n \rangle = 1740$ (left) and 14250 (right). Solid lines show the fits based on which the biexponential or oscillatory dynamics are identified; for details on fitting see Methods. **b**, Temporal evolution of the photon number response in the condensate after a weak pulsed perturbation of the reservoir at the same $\langle n \rangle$ as in **a**. Similarly, the dynamics is biexponential or oscillatory as determined by fitting the linear expression for $R(t)$ shown as solid lines. Insets show scaled derivative of fitted response dR/dt and fitted $g^{(2)}(\tau) - 1$, vertically shifted for clarity. Fit parameters in **a** $\delta_{\text{fluct}} = \{0.91(13), 0.33(3)\}\text{ns}^{-1}$ and $\omega_{0,\text{fluct}} = \{0.83(6), 1.45(2)\}\text{ns}^{-1}$, in **b** $\delta_{\text{resp}} = \{0.81(32), 0.39(2)\}\text{ns}^{-1}$ and $\omega_{0,\text{resp}} = \{0.75(14), 1.52(2)\}\text{ns}^{-1}$. Error bars show standard statistical errors.

To probe the response and fluctuation dynamics, we first prepare a steady-state photon BEC by quasi-cw optical pumping of the dye molecule reservoir over 600 ns at 532 nm wavelength, see Figs. 1(b),(c). After roughly 200 ns, a short laser pulse of 28 ps duration (also at 532 nm) irradiates the microcavity to perturb the reservoir. Part of the emission leaking from the microcavity is filtered in momentum space and for polarisation, and the photon number evolution in the transmitted condensate mode is recorded using a photomultiplier (Methods). Figure 1(d) shows an example of the condensate evolution after averaging over many time traces, from which the response dynamics is visible in a time window of 20 ns after the perturbation. The fluctuation dynamics is determined by analysing the second-order correlations $g^{(2)}(\tau)$ from individual time traces. Throughout all measurements the system parameters $B_{\text{em}} = 25 \text{ kHz}$, $\hbar\Delta = -3.87k_{\text{B}}T$, $\Gamma_{\text{sp}} = 250 \text{ MHz}$ remain fixed, while the total molecule number $M = 5.4(15) \cdot 10^9$, and mirror transmission $\kappa = 4.9(10) \text{ GHz}$ are obtained from fits to the data (Methods).

Figure 2 shows measured second-order correlation functions $g^{(2)}(\tau)$ and photon number responses $R(t)$ along with fits for two steady-state photon numbers $\langle n \rangle$, realised by varying the quasi-cw pump power. We are first interested in the linear response of the photon condensate, so we use only relatively small perturbation pulse powers that weakly change

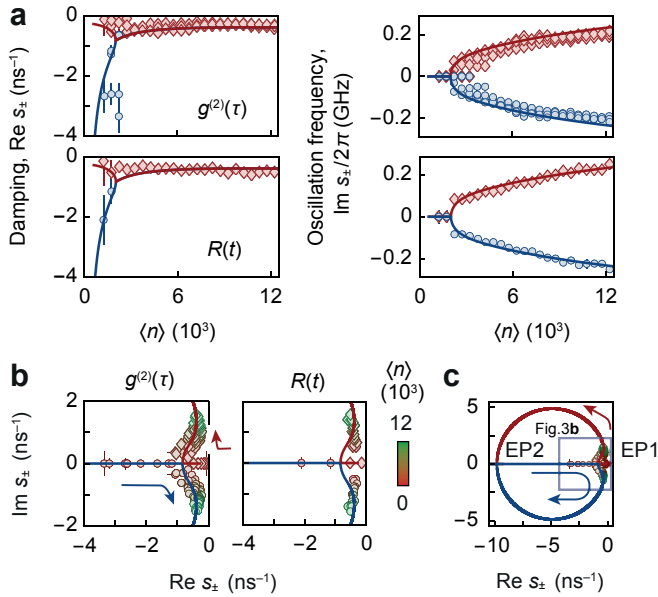


Fig. 3. Regression theorem for weak perturbations. **a**, Damping rate $\text{Re}(s_{\pm})$ and oscillation frequency $\text{Im}(s_{\pm})/(2\pi)$ of second-order correlations (top) and perturbation response (bottom) versus $\langle n \rangle$. Red and blue colours indicate s_+ and s_- , respectively. Solid lines give theory prediction. **b**, Complex eigenvalue spectrum near the exceptional point for $g^{(2)}(\tau)$ (left panel) and $R(t)$ (right), along with theory (solid). The eigenvalues evolve as a function of $\langle n \rangle$, as indicated by arrows and symbol colour, from being real to complex-valued. **c**, Imaginary gap opening at exceptional point (EP1) and theoretically predicted gap closing for larger $\langle n \rangle \approx 7.6 \cdot 10^5$ (EP2). Error bars show standard fitting errors.

the condensate population by $\delta n(t_{\max})/\langle n \rangle = 0.31(7)$ on average, where t_{\max} denotes the time when the photon population has reached its maximum. Accordingly, the response data is fitted using the linearized form of $R(t)$ discussed above. While generically $g^{(2)}(\tau) = 1$ and $R(t) = 0$ are found for large τ and t , both data sets display distinct dynamics. For small $\langle n \rangle = 1740$, both $g^{(2)}(\tau)$ and $R(t)$ decay biexponentially, while for large $\langle n \rangle = 14250$ a damped oscillation of the fluctuations and the response is observed. The quantitative agreement of the dynamics in Fig. 2 is seen in the parameters δ, ω_0 which determine the eigenvalues s_{\pm} . This gives evidence that the intrinsic number fluctuations and the response dynamics of the photon condensate to an external perturbation of the reservoir are governed by the same microscopic physics. Qualitatively, the agreement is more clearly visible when forming the derivative of the fitted response $dR(t)/dt$, see the inset of Fig. 2b, which well resembles the corresponding fit for $g^{(2)}(\tau)$ from Fig. 2a. Note that the biexponential and oscillatory dynamics are distinctly characterised by real and complex-valued s_{\pm} , respectively, which allows to identify a transition point between both dynamical regimes at the degeneracy $s_+ = s_-$, known as an exceptional point [28].

To systematically verify the universal relationship between $R(t)$ and $g^{(2)}(\tau)$ in the linear response regime, we next study the eigenvalues s_{\pm} of the condensate dynamics as a func-

tion of the steady-state population $\langle n \rangle$. Figure 3a shows the measured damping rate $\text{Re}(s_{\pm})$ and oscillation frequency $\text{Im}(s_{\pm})/(2\pi)$ for the response and fluctuation dynamics (symbols), respectively, along with the eigenvalue prediction from eq. (1) (lines). Note that for $R(t)$, we only show data for the smallest experimentally realised perturbation powers (as in Fig. 2), where the linear model is expected to be well applicable. At photon numbers below the one at the exceptional point $\langle n \rangle_{\text{EP}} \approx 2000$, two branches of damping constants with vanishing oscillation frequency indicate the biexponential regime, while for larger photon numbers the observed merging of $\text{Re}(s_{\pm})$ and bifurcation in $\text{Im}(s_{\pm})$ highlight the regime of oscillatory dynamics.

Figure 3a can be understood as a nonequilibrium phase diagram of the photon dynamics, where $\langle n \rangle$ presents a control parameter to tune between both phases. The associated opening of an imaginary gap at the phase transition is visible in the complex eigenvalue spectra of $g^{(2)}(\tau)$ and $R(t)$ in Fig. 3b; symbol colours indicate the photon number, which parametrises the spectral trajectory of $s_{\pm}(\langle n \rangle)$. As the photon number is increased, the real-valued s_{\pm} (biexponential dynamics) move from $\{\text{Re}(s_+), \text{Im}(s_+)\} = \{-\infty, 0\}$ and $\{\text{Re}(s_-), \text{Im}(s_-)\} = \{0, 0\}$ along the real axis and coalesce at the exceptional point $\{\text{Re}(s_{\pm}), \text{Im}(s_{\pm})\} \approx \{-0.8, 0\} \text{ns}^{-1}$. As $\langle n \rangle$ is increased further, the eigenvalues s_{\pm} separate again and move into the imaginary plane (oscillatory dynamics). The agreement between the measured linear response, the fluctuation dynamics, and the theory prediction provides an experimental benchmark for the regression theorem in optical quantum gases. Interestingly, for large condensate populations currently not accessible in the experiment and shown in Fig. 3c, theory hints at a second exceptional point in the condensate dynamics. Physically, the re-emerging biexponential phase results from competing the scaling of $\delta \sim \langle n \rangle$ and $\omega \sim \sqrt{\langle n \rangle}$, such that oscillations are damped out in the limit of very large $\langle n \rangle$.

We next generalize our study of the regression theorem to the nonlinear regime by successively increasing the reservoir perturbation strength m_0 induced by the pulse laser. Figure 4a shows complex eigenvalue spectra $s_{\pm}(\langle n \rangle)$ obtained from fitting either the linear (top row) or nonlinear (bottom) expression of $R(t)$ to the recorded condensate time traces. While for the weak perturbation the linear and nonlinear analysis yield similar results, a deviation from linear response theory is observed for the larger perturbations, as highlighted by the orange shading. In contrast, fitting the nonlinear expression in eq. (1) restores the eigenvalue spectrum of the response dynamics to agree well with the theoretical prediction for the fluctuation dynamics. This improvement demonstrates that the strongly perturbed photon condensate exhibits a pronounced nonlinearity, which occurs in our system when the molecule reservoir is saturated: almost all the excitations that are introduced by the perturbation pulse are then converted into photons leading to a large relative variation of the photon number, that activates the nonlinearity in the stimulated emission and absorption dynamics. Figure 4b shows the residuals

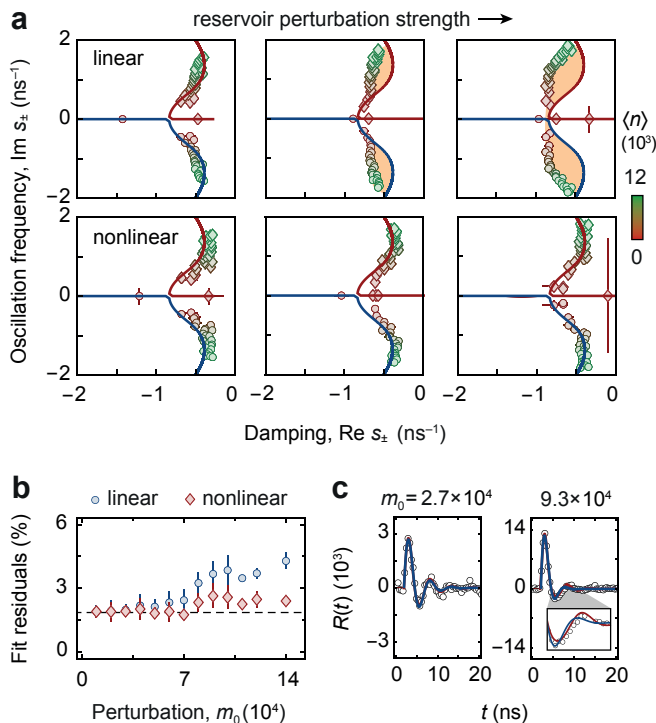


Fig. 4. Nonlinear BEC response. **a**, Complex eigenvalue spectra for increased reservoir perturbations with $\delta n(t_{\max})/\langle n \rangle = \{0.59(10), 1.15(23), 1.25(25)\}$ and $m_0 = \{5(2), 9(1), 11(3)\} \cdot 10^4$. Top row: Eigenvalues s_{\pm} (data points) obtained from a linear fit gradually deviate from theory (solid lines) due to a saturation-induced nonlinearity (shaded area). Bottom: s_{\pm} extracted from the nonlinear fit restore the agreement with theory, demonstrating a beyond-linear regression relation. **b**, Residuals of linear and nonlinear fits versus increasing m_0 averaged for $\langle n \rangle \geq 4000$ indicate the improved accuracy of the nonlinear fit. Dashed line gives noise floor. **c**, Photon response after a weak (left) and strong perturbation (right) for $\langle n \rangle \approx 8250$, along with linear (blue line) and nonlinear (red) fits. Error bars show standard fitting errors in **a**, and standard statistical errors in **b**.

$(\sqrt{\sum_i (R_{\text{exp},i} - R_{\text{fit},i})^2 / N}) / \langle n \rangle$ of the linear and nonlinear fit as the initial pulse perturbation is increased. Here, N denotes the number of recorded samples. Both the linear and the nonlinear fit yield similar and small residuals for weak perturbations below $m_0 \approx 5 \cdot 10^4$ (extracted from the fit), confirming that the condensate-reservoir coupling can here be well described by linear dynamics. Beyond this value, however, the residuals exhibit a splitting. While the linear fit performs significantly worse (*i.e.*, the residuals grow), the nonlinear fit residuals remain close to their initial values, demonstrating that the nonlinear expression is more accurate in describing the response dynamics of the photon condensate in the case of relatively strong perturbations of the molecule reservoir. Despite the improved accuracy of the nonlinear model, we note that for even stronger perturbations, as theoretically expected, also our nonlinear description gradually loses its accuracy due to a linearisation in m (Methods).

Finally, the nonlinearity of the photon condensate coupled

to the molecule reservoir is directly visible when we compare the measured oscillatory response $R(t)$ in Fig. 4c for a weak and a strong perturbation strength with $m_0 \approx 2.7 \cdot 10^4$ and $m_0 \approx 9.3 \cdot 10^4$, respectively. The solid lines show fits based on the linearized and full nonlinear expressions. For the weak perturbation, we find both models to describe the experimental data equally well. For the larger perturbation strength, the measurement is more accurately fitted by the nonlinear expression, as highlighted in the zoom-in view on the 5 to 12 ns time range in the inset of Fig. 4c.

To conclude, we have measured the response dynamics of a photon Bose-Einstein condensate after a sudden perturbation of the reservoir, which before the perturbation forms an equilibrium steady-state with the condensate. Comparing the response dynamics with the number fluctuations has enabled the experimental verification of the regression theorem for optical quantum gases. Specifically, we have identified a nonlinear response of the BEC at strong driving. Here an extended regression theorem of the form $g^{(2)}(\tau) - 1 \propto d/dt \ln[1 + R(t)/\langle n \rangle]$ holds, which in the limit of small perturbations agrees with the conventional linear form. For the future, the demonstrated scheme to perturb photon condensates constitutes a novel tool for exploring Kibble-Zurek dynamics [39, 40], or vortex turbulence [7, 35] in optical quantum gases in tailored potentials [41, 42]. An extension of the reported single BEC-bath oscillator system to arrays of coherently coupled condensates linked with local reservoirs will enable the exploration of reservoir-induced transport dynamics and open-system topological states [36, 37]. Our findings also pave the way for studies of the time-dependent fluctuation-dissipation relation in photon condensates, which so far have only been confirmed for static reactive response functions [29].

ACKNOWLEDGEMENTS

We thank F. E. Öztürk for assistance in early experimental stages; and C. Maes, R. Panico, L. Espert Miranda, N. Longen and A. Redmann for fruitful discussions. This work was financially supported by the DFG within SFB/TR 185 (277625399) and the Cluster of Excellence ML4Q (EXC 2004/1–390534769), and by the DLR with funds provided by the BMWi (50WM1859). J. S. acknowledges support by the EU (ERC, TopoGrand, 101040409), and V. G. and M. Wo. by FWO-Vlaanderen (G061820N).

* Present address: Leibniz Institute of Photonic Technology, Albert-Einstein-Str. 9, 07745 Jena, Germany

† schmitt@iap.uni-bonn.de

- [1] R. Kubo, Statistical-mechanical theory of irreversible processes. I. General theory and simple applications to magnetic and conduction problems, *J. Phys. Soc. Japan* **12**, 570 (1957).
- [2] V. Lucarini, J. Saarinen, K. Peiponen, and E. Vartiainen, *Kramers-Kronig Relations in Optical Materials Research*, Springer Series in Optical Sciences (Springer, 2005).

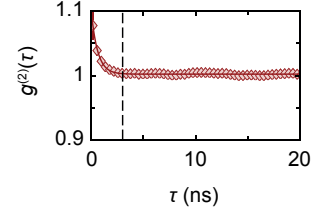
- [3] D. Chandler, *Introduction to Modern Statistical Mechanics* (Oxford University Press, 1987).
- [4] P. Christodoulou, M. Gałka, N. Dogra, R. Lopes, J. Schmitt, and Z. Hadzibabic, Observation of first and second sound in a BKT superfluid, *Nature* **594**, 191 (2021).
- [5] R. W. Boyd, The nonlinear optical susceptibility, in *Nonlinear Optics* (Elsevier, 2008).
- [6] M. Gałka, P. Christodoulou, M. Gazo, A. Karailiev, N. Dogra, J. Schmitt, and Z. Hadzibabic, Emergence of isotropy and dynamic scaling in 2d wave turbulence in a homogeneous bose gas, *Phys. Rev. Lett.* **129**, 190402 (2022).
- [7] R. Panico, P. Comaron, M. Matuszewski, A. S. Lanotte, D. Trypogeorgos, G. Gigli, M. D. Giorgi, V. Ardizzone, D. Sanvitto, and D. Ballarini, Onset of vortex clustering and inverse energy cascade in dissipative quantum fluids, *Nat. Photon.* **17**, 451 (2023).
- [8] R. Kubo, The fluctuation-dissipation theorem, *Rep. Prog. Phys.* **29**, 255 (1966).
- [9] L. Onsager, Reciprocal relations in irreversible processes. I., *Phys. Rev.* **37**, 405 (1931).
- [10] M. Lax, Formal theory of quantum fluctuations from a driven state, *Phys. Rev.* **129**, 2342 (1963).
- [11] G. Agarwal, Fluctuation-dissipation theorems for systems in non-thermal equilibrium and application to laser light, *Phys. Lett. A* **38**, 93 (1972).
- [12] M. O. Scully and M. S. Zubairy, *Quantum Optics* (Cambridge University Press, Oxford, 1997).
- [13] P. Hänggi, Stochastic processes. II. Response theory and fluctuation theorems, *Helv. Phys. Acta* **51**, 202 (1978).
- [14] M. Lax, The lax–onsager regression ‘theorem’ revisited, *Opt. Commun.* **179**, 463 (2000).
- [15] M. Baiesi, C. Maes, and B. Wynants, Fluctuations and response of nonequilibrium states, *Phys. Rev. Lett.* **103**, 010602 (2009).
- [16] C. Maes, Response theory: A trajectory-based approach, *Front. Phys.* **8**, 229 (2020).
- [17] J. Klatt, M. B. Farías, D. A. R. Dalvit, and S. Y. Buhmann, Quantum friction in arbitrarily directed motion, *Phys. Rev. A* **95**, 052510 (2017).
- [18] U. Basu, M. Krüger, A. Lazarescu, and C. Maes, Frenetic aspects of second order response, *Phys. Chem. Chem. Phys.* **17**, 6653 (2015).
- [19] D. G. Miller, Thermodynamics of irreversible processes. The experimental verification of the Onsager reciprocal relations., *Chem. Rev.* **60**, 15 (1960).
- [20] A. D. Avery and B. L. Zink, Peltier cooling and Onsager reciprocity in ferromagnetic thin films, *Phys. Rev. Lett.* **111**, 126602 (2013).
- [21] I. Bloch, J. Dalibard, and W. Zwerger, Many-body physics with ultracold gases, *Rev. Mod. Phys.* **80**, 885 (2008).
- [22] J. Bloch, I. Carusotto, and M. Wouters, Non-equilibrium Bose–Einstein condensation in photonic systems, *Nat. Rev. Phys.* **4**, 470–488 (2022).
- [23] D. Hunger, S. Camerer, T. W. Hänsch, D. König, J. P. Kotthaus, J. Reichel, and P. Treutlein, Resonant coupling of a Bose-Einstein condensate to a micromechanical oscillator, *Phys. Rev. Lett.* **104**, 143002 (2010).
- [24] J. Klaers, J. Schmitt, F. Vewinger, and M. Weitz, Bose–Einstein condensation of photons in an optical microcavity, *Nature* **468**, 545 (2010).
- [25] J. Marelic and R. A. Nyman, Experimental evidence for inhomogeneous pumping and energy-dependent effects in photon Bose-Einstein condensation, *Phys. Rev. A* **91**, 033813 (2015).
- [26] S. Greveling, K. L. Perrier, and D. van Oosten, Density distribution of a Bose-Einstein condensate of photons in a dye-filled microcavity, *Phys. Rev. A* **98**, 013810 (2018).
- [27] J. Schmitt, T. Damm, D. Dung, F. Vewinger, J. Klaers, and M. Weitz, Observation of grand-canonical number statistics in a photon Bose-Einstein condensate, *Phys. Rev. Lett.* **112**, 030401 (2014).
- [28] F. E. Öztürk, T. Lappe, G. Hellmann, J. Schmitt, J. Klaers, F. Vewinger, and M. Weitz, Observation of a non-Hermitian phase transition in an optical quantum gas, *Science* **372**, 88 (2021).
- [29] F. E. Öztürk, F. Vewinger, M. Weitz, and J. Schmitt, Fluctuation-dissipation relation for a Bose-Einstein condensate of photons, *Phys. Rev. Lett.* **130**, 033602 (2023).
- [30] J. Schmitt, T. Damm, D. Dung, F. Vewinger, J. Klaers, and M. Weitz, Thermalization kinetics of light: From laser dynamics to equilibrium condensation of photons, *Phys. Rev. A* **92**, 011602 (2015).
- [31] B. T. Walker, J. D. Rodrigues, H. S. Dhar, R. F. Oulton, F. Mintert, and R. A. Nyman, Non-stationary statistics and formation jitter in transient photon condensation, *Nat. Commun.* **11**, 1390 (2020).
- [32] J. Schmitt, Dynamics and correlations of a Bose–Einstein condensate of photons, *J. Phys. B: At. Mol. Opt. Phys.* **51**, 173001 (2018).
- [33] W. Verstraelen and M. Wouters, Temporal coherence of a photon condensate: A quantum trajectory description, *Phys. Rev. A* **100**, 013804 (2019).
- [34] A. Opala, M. Pieczarka, and M. Matuszewski, Theory of relaxation oscillations in exciton-polariton condensates, *Phys. Rev. B* **98**, 195312 (2018).
- [35] V. N. Gladilin and M. Wouters, Vortices in nonequilibrium photon condensates, *Phys. Rev. Lett.* **125**, 215301 (2020).
- [36] H. Wetter, M. Fleischhauer, S. Linden, and J. Schmitt, Observation of a topological edge state stabilized by dissipation, *Phys. Rev. Lett.* **131**, 083801 (2023).
- [37] L. Garbe, Y. Minoguchi, J. Huber, and P. Rabl, The bosonic skin effect: boundary condensation in asymmetric transport, arXiv:2301.11339 10.48550/arXiv.2301.11339 (2023).
- [38] P. Kirton and J. Keeling, Thermalization and breakdown of thermalization in photon condensates, *Phys. Rev. A* **91**, 033826 (2015).
- [39] M. Kulczykowski and M. Matuszewski, Phase ordering kinetics of a nonequilibrium exciton-polariton condensate, *Phys. Rev. B* **95**, 075306 (2017).
- [40] P. Comaron, G. Dagvadorj, A. Zamora, I. Carusotto, N. P. Proukakis, and M. H. Szymańska, Dynamical critical exponents in driven-dissipative quantum systems, *Phys. Rev. Lett.* **121**, 095302 (2018).
- [41] D. Dung, C. Kurtscheid, T. Damm, J. Schmitt, F. Vewinger, M. Weitz, and J. Klaers, Variable potentials for thermalized light and coupled condensates, *Nat. Photon.* **11**, 565 (2017).
- [42] E. Busley, L. E. Miranda, A. Redmann, C. Kurtscheid, K. K. Umesh, F. Vewinger, M. Weitz, and J. Schmitt, Compressibility and the equation of state of an optical quantum gas in a box, *Science* **375**, 1403 (2022).

METHODS

EXPERIMENTAL METHODS AND CALIBRATIONS

For the steady-state excitation of the photon Bose-Einstein condensate inside the dye-filled microcavity, we use a cw laser at 532 nm wavelength (Coherent Verdi 15G). To minimize bleaching of the dye medium (Rhodamine 6G solved in ethylene glycol, concentration 1 mmol L⁻¹ and zero-phonon line $\omega_{zpl} = 2\pi \times 550$ THz) as well as pumping to nonradiative triplet states, the pump beam emission is temporally chopped into pulses of 600 ns at a repetition rate of 50 Hz by acousto-optic modulators. During the steady state, a mode-locked laser pulse of 28 ps duration at 532 nm wavelength (EKSPLA PL 2201) is irradiated onto the dye-filled cavity at the same repetition rate, *i.e.*, there is one perturbation pulse during the 600 ns-long steady-state. The laser pulse instantaneously perturbs the number of excited dye molecules, and consequently also drives the photon condensate out of its steady state. The residual condensate emission transmitted through both cavity mirrors is used for the analysis of the experiment. On one side of the cavity, a microscope objective (Mitutoyo MY10X-803) collects the emission to measure the spectral distribution and the spatial intensity distribution of the photon gas. The cavity length is actively stabilized by monitoring the cutoff wavelength behind an Echelle grating on an EMCCD camera (Andor iXon 897). On the opposite cavity side, the cavity emission is filtered by truncating high-momentum states of the photon gas using an iris in the far field. The filtered condensate mode is detected using a photomultiplier (PHOTEK PMT 210) with a temporal resolution of 150 ps FWHM that is sampled by an oscilloscope (Tektronix DPO7354C) operated at 20 GSa/s sampling rate with a 2 GHz bandwidth. To calibrate the condensate population $\langle n \rangle$ against the recorded PMT voltage, the photon gas spectrum is fitted with a Bose-Einstein distribution [24].

To exclude systematic sources of errors in our PMT-based measurements of the temporal second-order correlations $g^{(2)}(\tau)$, we perform a benchmark with a HeNe laser at 632.8 nm wavelength, see Extended Data Fig. 1. For the coherent source, one expects $g^{(2)}(\tau) = 1$ for all time delays. However, the obtained signal shows $g^{(2)}(\tau) > 1$ up to $\tau \approx 3$ ns, an observation which we attribute to electronic noise in the detection system. To avoid a misinterpretation of the data arising from this artefact, we exclude data points at $\tau \leq 3$ ns from the analysis of the correlation dynamics. Moreover, radiofrequency noise collected by our detection system (*e.g.*, during pulse picking in the pulse laser system) is visible in the averaged time traces of the photon condensate response at the time of the pulse emission. To mitigate this, an optical delay line has been implemented to shift the pulse arrival time at the microcavity with respect to the noise signal. The delay line is realised by a cavity of 24 m length (corresponding to a time delay of 80 ns), which is traversed by the pulse 6 times. To that end, all response measurements can be per-



Extended Data Fig. 1. Second-order correlations $g^{(2)}(\tau)$ measured for HeNe laser. The measurement is used to benchmark the photomultiplier-based detection method of $g^{(2)}(\tau)$. The ‘fake’ bunching signal at $\tau < 3$ ns (dashed line) is not caused by actual photon bunching; instead, it is attributed to electronic noise from the single-detector measurement system. The early-time data points are thus disregarded for the analysis of the photon dynamics. Solid line shows exponential fit with time constant of 0.6 ns.

formed in a temporal region free of residual radiofrequency-induced noise.

THEORETICAL MODEL

Using the Kennard-Stepanov relation for the absorption and emission rates of the dye medium, the rate equation for the number of photons n can be rewritten as

$$\frac{dn}{dt} = B_{\text{em}}n \left[M_{\uparrow} \left(1 + \frac{1}{n} + e^{\hbar\Delta/k_{\text{B}}T} \right) - M e^{\hbar\Delta/k_{\text{B}}T} \right] - \kappa n. \quad (\text{S1})$$

We represent the number of excited molecules as

$$M_{\uparrow} = M_{\uparrow,n} + m, \quad (\text{S2})$$

where

$$M_{\uparrow,n} = \frac{M + \kappa e^{-\hbar\Delta/k_{\text{B}}T} / B_{\text{em}}}{1 + e^{-\hbar\Delta/k_{\text{B}}T} (1 + 1/\langle n \rangle)} \quad (\text{S3})$$

is the number of excited molecules, which corresponds to the steady state with the average photon number equal to n . Then for the experimentally relevant case $n \gg 1$, eq. (S1) takes the form

$$\frac{dn}{dt} = B_{\text{em}}(1 + e^{\hbar\Delta/k_{\text{B}}T})mn, \quad (\text{S4})$$

which leads to the following nonlinear relation between $m(t)$ and the corresponding evolution of the photon number, starting from its value $\langle n \rangle$ at $t = 0$:

$$n(t) = \langle n \rangle \exp \left[B_{\text{em}}(1 + e^{\hbar\Delta/k_{\text{B}}T}) \int_0^t m(t') dt' \right]. \quad (\text{S5})$$

To describe the dynamics of $m(t)$ initiated by a sudden perturbation of the excited molecule number at $t = 0$, we utilize the rate equation for $X \equiv M_{\uparrow,n} + m + n$ with $P = P_0$,

$$\frac{dM_{\uparrow,n}}{dt} + \frac{dm}{dt} + \frac{dn}{dt} = -\Gamma_{\text{sp}}(M_{\uparrow,n} + m - \langle M_{\uparrow} \rangle) - \kappa(n - \langle n \rangle), \quad (\text{S6})$$

where $\langle M_{\uparrow} \rangle \equiv M_{\uparrow, \langle n \rangle}$ and

$$\frac{dM_{\uparrow, n}}{dt} = \frac{dM_{\uparrow, n}}{dn} \frac{dn}{dt} = \frac{M_{\text{eff}}}{n^2} \frac{dn}{dt} \quad (\text{S7})$$

with

$$M_{\text{eff}} = \frac{M + \kappa e^{\hbar\Delta/k_{\text{B}}T}/B_{\text{em}}}{2[\cosh(\hbar\Delta/k_{\text{B}}T) + 1]}. \quad (\text{S8})$$

Inserting eqns. (S3), (S5) and (S7) into eq. (S6), one obtains a rather cumbersome nonlinear differential equation for $\int_0^t m dt'$, which, in general, cannot be solved analytically. To proceed further, we assume that m is relatively small and hence it can be estimated from the linearized version of the aforementioned equation

$$\frac{dm}{dt} + 2m\delta + \omega_0^2 \int_0^t m dt' = 0, \quad (\text{S9})$$

where

$$\delta = \frac{B_{\text{em}}}{2} \left(1 + e^{\hbar\Delta/k_{\text{B}}T}\right) \left(\frac{M_{\text{eff}}}{\langle n \rangle} + \langle n \rangle\right) + \frac{\Gamma_{\text{sp}}}{2}, \quad (\text{S10})$$

$$\omega_0^2 = \langle n \rangle B_{\text{em}} \left(1 + e^{\hbar\Delta/k_{\text{B}}T}\right) \left(\kappa + \frac{M_{\text{eff}}\Gamma_{\text{sp}}}{\langle n \rangle^2}\right). \quad (\text{S11})$$

Equation (S9) has the solution

$$\int_0^t m dt' = m_0 \frac{e^{s_+t} - e^{s_-t}}{s_+ - s_-} \quad (\text{S12})$$

with

$$s_{\pm} = -\delta \pm \sqrt{\delta^2 - \omega_0^2}. \quad (\text{S13})$$

Here, $m_0 = m(0)$ is the number of molecules excited by the initial perturbation. Inserting eq. (S12) into (S5), we can express the time dependence of the photon number in an explicit form:

$$n(t) = \langle n \rangle \exp \left[B_{\text{em}} (1 + e^{\hbar\Delta/k_{\text{B}}T}) m_0 \frac{e^{s_+t} - e^{s_-t}}{s_+ - s_-} \right] \quad (\text{S14})$$

RELATION BETWEEN $R(t)$ AND $g^{(2)}(t)$

The regression theorem implies that the response dynamics $RR(t) = n(t) - \langle n \rangle$ of the photon condensate after a perturbation of the molecule reservoir is related to the condensate's second-order coherence $g^{(2)}(t) = \langle n(t)n(0) \rangle / \langle n \rangle^2$ by $g^{(2)}(t) - 1 \propto dR(t)/dt$. In linear response, for small deviations around the mean photon number $n = \langle n \rangle + \Delta n$ and excitation number $X = \langle X \rangle + \Delta X$, we have the following equations of motion for the time evolution after the system has been perturbed:

$$\frac{d}{dt} \Delta X = -\kappa \Delta n \quad (\text{S15})$$

$$\frac{d}{dt} \Delta n = -\Gamma \Delta n + \frac{\delta n^2}{M_{\text{eff}}} \Gamma \Delta X, \quad (\text{S16})$$

with coefficient $\delta n^2 = M_{\text{eff}} \langle n \rangle^2 / (M_{\text{eff}} + \langle n \rangle^2)$ and $\Gamma(\langle n \rangle) = B_{\text{em}} [1 + \exp(\hbar\Delta/k_{\text{B}}T)] (M_{\text{eff}}/\langle n \rangle + \langle n \rangle)$. The first equation expresses that excitations are only lost through cavity losses (we here neglect losses from molecule decay). The second equation expresses (i) that deviations in the photon density at constant X relax at the rate Γ and (ii) that changes in X lead to a change in the photon number. When an additional laser pulse is applied to perturb the molecules, the system gets initial conditions $\Delta X = \delta X, \Delta n = 0$ at time $t = 0$. The response to this perturbation is calculated from eqns. (S15) and (S16) and it corresponds to the linearisation of eq. (S14):

$$R(t) = \frac{\delta X \delta n^2}{M_{\text{eff}}} \Gamma \frac{e^{s_+t} - e^{s_-t}}{s_+ - s_-} \quad (\text{S17})$$

In order to compute the density-density correlator $G^{(2)}(t) = \langle n(t)n(0) \rangle - \langle n \rangle^2 = \langle \delta n(t) \delta n(0) \rangle$ with $\delta n(t) = n(t) - \langle n \rangle$ in the presence of losses, we can use the regression formula:

$$\langle \delta n(t) \delta n(0) \rangle = \langle \delta n(t) | \delta n_0 \rangle \delta n_0 \quad (\text{S18})$$

Here $\delta n(t) | \delta n_0$ is the average photon deviation starting from a deviation δn_0 at time $t = 0$. From eqns. (S15) and (S16) and for $\Delta n = \delta n_0, \Delta X = 0$ one finds

$$\delta n(t) | \delta n_0 = \delta n_0 \frac{s_+ e^{s_+t} - s_- e^{s_-t}}{s_+ - s_-} \quad (\text{S19})$$

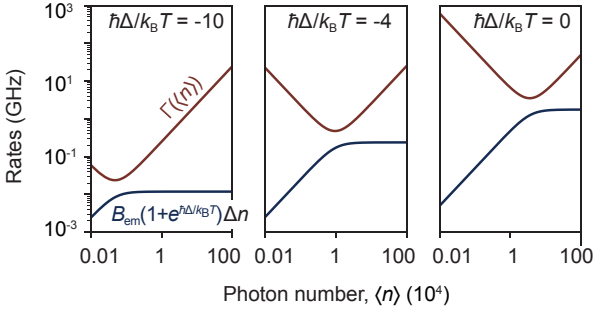
From eqns. (S18) and (S19), we then obtain

$$G^{(2)}(t) = \delta n_0^2 \frac{s_+ e^{s_+t} - s_- e^{s_-t}}{s_+ - s_-}. \quad (\text{S20})$$

This expression contains the same rates (and frequencies) as the response function eq. (S17) but does not show identical time dependence. From the derivation of the correlation function, one can see that a perturbation in the number of photons at constant X would give a density response with the same time dependence as $G^{(2)}(t)$. Such a perturbation is hard to implement experimentally. By comparing eqns. (S17) and (S20) one sees that the relation

$$G^{(2)}(t) = \frac{M_{\text{eff}}}{\delta X} \frac{1}{\Gamma} \frac{d}{dt} R(t) \quad (\text{S21})$$

holds. Using $G^{(2)}(t) = [g^{(2)}(t) - 1] \langle n \rangle^2$, this corresponds to the relation stated in the beginning of this section. In the case of an oscillating density response, the derivative implies that the correlation and response functions have a phase shift of $\pi/2$. Physically, this can be understood from the fact that an external laser pulse excites the molecules, which take some time to be converted into photons. This gives a delay for the response function with respect to the correlation function. In Fig. 2 one sees that the correlations show a minimum as a function of time while the response does not. The correlation function $G^{(2)}(t)$ must become negative as can be seen from the differential relation in eq. (S21) and $\Delta n(t \rightarrow \infty) = 0$ in the presence of losses. Physically, it is a consequence of a positive photon number fluctuation at some moment to imply larger losses, which reduces the expected photon number later on.



Extended Data Fig. 2. Linearity of grand canonical number fluctuations. Graphical comparison of rates from eq. (S23) for a photon condensate subject to reservoir-induced fluctuations for dye-cavity detunings $\hbar\Delta/k_B T = \{-10, -4, 0\}$. The linear fluctuation rate $\Gamma(\langle n \rangle)$ (red) exceeds the rate that would lead to nonlinear dynamics (blue) for all detunings and photon numbers. Correspondingly, the dynamics of reservoir-induced fluctuations are expected to be well described by linear equations, in agreement with the experiments.

LINEARITY OF FLUCTUATION DYNAMICS

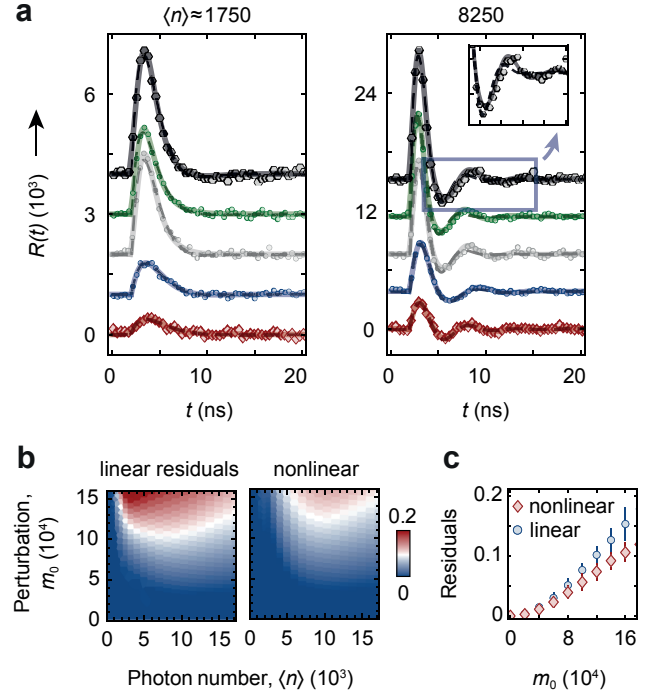
The particle number fluctuations and the corresponding second-order correlations of a photon Bose-Einstein condensate under grand canonical statistical conditions are governed by linear dynamics. Here a simple analytical reasoning for this statement is presented. The rate equations for the coupled photon-dye system can be employed to identify two competing rates, which determine whether nonlinear effects in the photon dynamics can or must not be neglected [32]. In the lossless case ($\kappa = \Gamma_{\text{sp}} = 0$), the rate equation for a photon number fluctuation away from its steady-state value reads

$$\frac{d\Delta n}{dt} = -B_{\text{em}}(1 + e^{\hbar\Delta/k_B T})\Delta n^2 - \Gamma\Delta n, \quad (\text{S22})$$

where $\Gamma(\langle n \rangle) = B_{\text{em}}(1 + e^{\hbar\Delta/k_B T})\left(\frac{M_{\text{eff}}^0}{\langle n \rangle} + \langle n \rangle\right)$, which corresponds to 2δ from eq. (S10) with the loss terms set to zero. The effective reservoir size M_{eff}^0 is given by eq. (S8) with $\kappa = 0$. For nonlinear effects to be relevant, $B_{\text{em}}[1 + \exp(\hbar\Delta/k_B T)]\Delta n \sim \Gamma$. Inserting δn (see Section ‘Relation of R(t) and g(2)(t)’), one has

$$B_{\text{em}}(1 + e^{\hbar\Delta/k_B T})\langle n \rangle \sqrt{\frac{M_{\text{eff}}^0}{M_{\text{eff}}^0 + \langle n \rangle^2}} \sim \Gamma(\langle n \rangle). \quad (\text{S23})$$

Extended Data Fig. 2 shows both rates as a function of $\langle n \rangle$ for different dye-cavity detunings, which changes the effective reservoir size. For all curves the second-order correlation rate (r.h.s) exceeds the nonlinear term (l.h.s.), meaning that a photon BEC driven by reservoir-induced fluctuations to good approximation always exhibits linear dynamics. Our experimental data in Figs. 2, 3 confirm this prediction, showing that the second-order correlation dynamics are well described by the derivative of the linear expansion of eq. (1).



Extended Data Fig. 3. Experimental time traces of nonlinear BEC response and accuracy of fit models. **a**, Experimental time traces of condensate response for increasing perturbation strength (bottom to top; vertically shifted) for $\langle n \rangle \approx 1750$ (left panel, biexponential) and 8250 (right, oscillatory) along with fits. While at moderate perturbations the data is well described by both linear (dashed) and nonlinear (solid) fits, the nonlinear model matches the observed dynamics better for strong perturbations. **b**, Crossover from linear (blue) to nonlinear (red) photon dynamics versus initial perturbation strength m_0 and photon number $\langle n \rangle$ as obtained from numerical simulations; colours indicate fit residuals. The nonlinear model exhibits generally smaller residuals and therefore matches the numerical data better especially in the limit of large perturbations. **c**, Numerically calculated residuals versus m_0 averaged for measurements with $\langle n \rangle \geq 4000$, showing the qualitatively same splitting behaviour as seen experimentally, see Fig. 4c.

FITTING OF EXPERIMENTAL DATA

To analyse the dynamics of the two-time correlations, we fit the second-order correlation data with

$$g^{(2)}(\tau) = a \frac{s_+ e^{s_+(\tau+\Delta\tau)} + s_- e^{s_-(\tau+\Delta\tau)}}{s_+ - s_-} + b, \quad (\text{S24})$$

where the eigenvalues of the dynamics are given by $s_{\pm} = -\delta \pm \sqrt{\delta^2 - \omega_0^2}$. Accordingly, for the response function in the nonlinear form we use the fit function

$$R_{\text{nl}}(t) = a \exp \left[b \frac{e^{s_+(t+\Delta\tau)} + e^{s_-(t+\Delta\tau)}}{s_+ - s_-} \right] - a \quad (\text{S25})$$

and for the linear form we fit

$$R_{\text{lin}}(t) = a' \frac{e^{s_+(t+\Delta\tau)} + e^{s_-(t+\Delta\tau)}}{s_+ - s_-} \quad (\text{S26})$$

The fit parameters δ and ω_0 resemble the damping constant and natural frequency of a harmonic oscillator; the time delay $\Delta\tau$ together with a, a', b are treated as free parameters for each fit. From the analysis of the condensate response dynamics, we find that both the linear and nonlinear fit can be used to describe the experimental data depending on the strength of the perturbation pulse, as shown in Figs. 4b,c of the main text and in the Extended Data Fig. 3.

For a quantitative comparison of the measured eigenvalues s_{\pm} with theory, several system parameters are required: On the one hand, the spontaneous molecule decay rate to unconfined optical modes $\Gamma_{\text{sp}} \approx 250$ MHz and the Einstein coefficient for emission $B_{\text{em}} = 25$ kHz at the dye-cavity detuning $\hbar\Delta/k_{\text{B}}T = -3.87$ (corresponding to a cutoff wavelength $\lambda_c = 570$ nm) are well known [28, 32]. The molecule number M and the cavity loss rate κ , on the other hand, need to be determined. For this, we compare our experimental results to a full numerical solution of the coupled photon-molecule rate equations and minimize the difference by varying the two parameters. To achieve this in a consistent way, all recorded time traces (*i.e.*, for all perturbation powers and all average photon numbers) are fitted simultaneously. This numerical

approach is motivated by the fact that even the nonlinear expression for the response dynamics in eq. (1) is not exact, because in its derivation m was assumed to be small. We obtain a molecule number $M = 5.4(15) \cdot 10^9$ and a cavity loss rate $\kappa = 4.9(10)$ GHz. The results are consistent with the corresponding values from analysing the second-order correlation function $g^{(2)}(\tau)$, $M = 6.6(7) \cdot 10^9$ and $\kappa = 6.6(10)$ GHz, which are obtained from fits of the linear expression in eq. (S24). As discussed above, this is justified because the fluctuation dynamics are expected to obey linear equations.

Finally, the numerical data allows us to cross-validate the fit results of the linear and nonlinear expressions to the experimental data. Extended Data Fig. 3b shows a map of linear and nonlinear residuals obtained from fitting numerically calculated data as a function of the photon number $\langle n \rangle$ and perturbation strength m_0 . Fitting the nonlinear expression always yields smaller residuals compared to the linear fit at the respective coordinates; Extended Data Fig. 3c shows the residuals versus m_0 when averaged for average photon numbers $\langle n \rangle \geq 4000$, which qualitatively agrees with the experimental observation of Fig. 4b that the nonlinear model can describe the data more accurately at large m_0 .